FEBS Letters 584 (2010) 3592–3600

journal homepage: www.FEBSLetters.org

miR-1/miR-206 regulate Hsp60 expression contributing to glucose-mediated apoptosis in cardiomyocytes

Zhi-Xin Shan [a], Qiu-Xiong Lin [a], Chun-Yu Deng [a], Jie-Ning Zhu [a], Li-Ping Mai [a], Ju-Li Liu [a], Yong-Heng Fu [a], Xiao-Ying Liu [a], Yang-Xin Li [b], You-Yi Zhang [c], Shu-Guang Lin [a], Xi-Yong Yu [a,*]

[a] Research Center of Guangdong General Hospital, Guangdong Provincial Cardiovascular Institute, Guangdong Academy of Medical Sciences, Guangzhou 510080, China
[b] Texas Heart Institute and University of Texas Health Science Center, 6770 Bertner Avenue, Houston, TX 77030, USA
[c] Institute of Vascular Medicine, Peking University Third Hospital, Beijing 100083, China

ARTICLE INFO

Article history:
Received 22 April 2010
Revised 12 July 2010
Accepted 15 July 2010
Available online 24 July 2010

Edited by Barry Halliwell

Keywords:
miR-1
miR-206
Hsp60
High glucose
H9c2 cell

ABSTRACT

Hsp60 is an important component of defense mechanisms against diabetic myocardial injury; however, the cause of Hsp60 reduction in the diabetic myocardium remains unknown. After stimulation of cardiomyocytes with high glucose in vivo and in vitro, significant up-regulation of miR-1/miR-206 and post-transcriptional modulation of Hsp 60 were observed. Serum response factor (SRF) and the MEK1/2 pathway were involved in miR-1 and miR-206 expression in cardiomyocytes. miR-1 and miR-206 regulated Hsp60 expression post-transcriptionally and accelerated cardiomyocyte apoptosis through Hsp60. These results revealed that miR-1 and miR-206 regulate Hsp60 expression, contributing to high glucose-mediated apoptosis in cardiomyocytes.

1. Introduction

High glucose-induced apoptosis of cardiomyocytes contributes to the development of diabetic complications [1,2]. Oxidative stress and altered calcium homeostasis are involved in high glucose-mediated cytotoxicity [3–5].

Heat shock proteins (Hsps) are a group of molecular chaperones that are capable of preventing protein damage and proteolysis. Hsp expression can be induced by heat, ischemia, hypoxia, ATP depletion, free radicals, and hypothermia [6]. Whereas 75–85% of Hsp60 is localized within the mitochondria, 15–20% is found in the cytosolic compartment [7]. Hsp60 modulates the Bcl-2 family of proteins, maintains the mitochondrial membrane electrochemical gradient, and prevents apoptotic cardiomyocyte death [6,8–10]. Thus, Hsp60 is an important component of defense mechanisms against diabetic myocardial injury. However, Hsp60 expression is significantly reduced in the diabetic myocardium [11–14], and the molecular mechanism for this reduction has yet to be elucidated.

MicroRNAs (miRNAs) are endogenous 20–23-nucleotide (nt)-containing small non-coding RNAs that negatively regulate gene expression in diverse biological and pathological processes, including cell differentiation, proliferation, apoptosis, heart disease, neurological disorders, and human cancers [15–19]. Recently, several studies have demonstrated that dysregulation of miRNAs is linked to diabetic cardiovascular dysfunction. For example, miR-221 is involved in c-kit-mediated endothelial cell migration under hyperglycemic conditions [20]. In cardiomyocytes, the activity of glucose transporter type 4 (GLUT4), the insulin-sensitive glucose transporter, can be modulated by miR-133 and miR-223 [21,22]. Among the known miRNAs, miR-1 is specifically expressed in cardiac and skeletal muscle cells [23–25]. Increased expression of miR-1 was found in the ventricular samples from diabetic patients [26]. In addition, high glucose-induced apoptosis of rat H9c2 cardiomyocytes via miR-1 and IGF-1 [27]. However, modulation of Hsp60 expression by miRNAs in diabetic cardiomyocytes remains to be determined.

In this study, we examined miR-1 and miR-206 expression in rat myocardium after onset of hyperglycemia and rat neonatal cardiomyocytes exposed to high glucose, and found that high glucose-induced significant up-regulation of miR-1 and miR-206. Furthermore, serum response factor (SRF) and the MEK1/2 pathway modulated miR-1 and miR-206 expression in cardiomyocytes. We also validated that rat miR-1 and miR-206 negatively regulated Hsp60 expression by directly targeting the 3′ untranslated region

* Corresponding author. Fax: +86 20 83769487.
E-mail address: yuxycn@hotmail.com (X.-Y. Yu).

0014-5793/$36.00
doi:10.1016/j.febslet.2010.07.027

(UTR) of Hsp60 mRNA. Thus, miR-1 and miR-206 repress Hsp60 expression, and up-regulation of miR-1 and miR-206 induced by high glucose may increase cardiomyocyte apoptosis.

2. Materials and methods

2.1. Streptozotocin (STZ)-induced rat diabetes model

This study conformed to the Guide for the Care and Use of Laboratory Animals published by the U.S. National Institutes of Health (NIH publication number 85-23, revised 1996). Sprague–Dawley (SD) rats weighing 245 ± 10 g (license number SCXK (YUE) 2004–0011; Department of Experimental Animal Research Center, Sun Yat-sen Medical College, Sun Yat-sen University, Guangzhou, China) were used.

STZ (55 mg/kg body weight, i.p.) was injected consecutively on alternate days into SD rats. The animals were fed a standard rodent diet and received water *ad libitum*. Blood glucose levels were monitored by tail-vein sampling. The diabetic rats were sacrificed at 4, 7, and 14 d after the onset of diabetes (random glucose >16.7 mM).

2.2. Echocardiography

Left ventricular (LV) function was assessed by transthoracic echocardiography, which was carried out 4, 7, and 14 d after the onset of diabetes. After administration of light general anesthesia, the rats underwent transthoracic two-dimensional (2D) guided M-mode echocardiography using a Technos MPX ultrasound system (ESAOTE, Italy). From the cardiac short axis (papillary level), LV end-diastolic dimension (LVDd), LV diameter at end-systole (LVDs), and ejection fraction (EF) were measured. Echocardiographic measurements included an average of at least three separate cardiac cycles.

2.3. TUNEL assay

Terminal deoxynucleotidyl transferase-mediated dUTP-nick-end labeling (TUNEL) was performed with a detection kit according to the instructions of DeadEnd™ Fluorometric TUNEL System (Promega, Madison, WI, USA). Briefly, heart tissue sections or H9C2 cells were fixed with 4% methanol-free formaldehyde at 4 °C for 25 min. Heart tissue sections were permeabilized with 20 μg/ml Proteinase K; H9C2 cells were permeabilized with 0.2% Triton X-100. After incubation with equilibration buffer (200 mM potassium cacodylate, 25 mM Tris–HCl, 0.2 mM DTT, 0.25 mg/ml BSA, 2.5 mM cobalt chloride, pH 6.6), DNA strand breaks in the apoptotic cells were labeled with fluorescein-12-dUTP. DAPI or Hoeshst was used to stain the nuclei of all cells, and fluorescence microscopy analysis followed. The percentage of TUNEL-positive cells was determined by counting approximately 200 cells per field in five different visual fields.

2.4. Construction of rat miR-1, miR-206, Hsp60 shRNA, and SRF shRNA expression plasmids

Rat miR-1 and miR-206 DNA fragments were PCR-amplified from SD rat genomic DNA after which they were introduced into pcDNA3.1 (Invitrogen, Carlsbad, CA USA) to construct pcDNA3-miR-1 and pcDNA3-miR-206 plasmids, respectively [28]. The target sequence of miR155-based rat *Hsp60* shRNA corresponds to the *Hsp60* gene (GenBank Accession number: NM_022229) sequence 5′-AGGTGTGATGTTGGCTGTTGA-3′, and the target sequence of miR155-based rat *SRF* shRNA corresponds to the *SRF* gene (GenBank Accession number: NM_001109302) sequence 5′-GAAGATCAAGATGGAGTTCAT-3′. *Hsp60*/miR155-shRNA and *SRF*/miR155-shRNA expression cassettes were prepared and introduced into pcDNA3.1 vector to construct pcDNA3-*Hsp60*/miR155-shRNA and pcDNA3-*SRF*/miR155-shRNA plasmids according to our previous report, respectively [29].

2.5. Dual Luciferase assay for Hsp60 target identification

Using the Targetscan program (www.targetscan.org/cgi-bin), one region (5′-AATAAAGACATTTGTACATTCCT-3′), was predicted to be the potential binding site of rat miR-1 and miR-206 in the 3′-untranslated region of the rat *Hsp60* gene. To anneal the double-strand DNA containing the above region, the following two oligonucleotides were synthesized: 5′-CTAGATTGAATAAAGACAT TTGTACATTCCTGATGCTGGGTGCAAGAGCCAG-3′ and 5′-AATTCTGG CTCTTGCACCCAGCATCAGGAATGTACAAATGTCTTTATTCAAT-3′. The annealed double-stranded DNA fragment was introduced into the *Xba* I and *Eco*R I sites (the additional *EcoR* I site was contained in the engineered pGL3-promoter vector) at the 3′ end of the firefly luciferine gene in the pGL3-promoter vector (Promega) to construct pGL3-*Hsp60* bs. Using a site-directed mutagenesis kit (TransGen, Beijing, China), the CATTC in the binding site for miR-1/miR-206 in pGL3-*Hsp60* bs was replaced with GTAAG to construct pGL3-*Hsp60*-MUT bs.

Human embryonic kidney (HEK) 293 cells (3×10^5 cells per well) were plated in 12-well plates 24 h before transfection. Cells were co-transfected with 200 ng of pGL3- *Hsp60* bs or pGL3-*Hsp*60-MUT bs, 1 μg of pcDNA3-miR-1 or pcDNA3-miR-206, and 20 ng of pRL-TK (Promega). pRL-TK, which expresses *Renilla* luciferase (RL) was added as an internal control for cell viability and transfection efficiency. Activities of firefly luciferase and RL were measured 48 h after transfection, and the relative ratio of the firefly luciferase/RL was used to determine Hsp60 knock-down mediated by miR-1 and miR-206.

2.6. Dual luciferase assay for miR-1 and miR-206 transcription activity detections

The transcription factor, SRF, modulates miR-1 expression in cardiomyocytes [30]. According to 60-kb 5′UTR sequences of rno-miR-1 (miRBase MI0003489, Chromosome 18: 2191,671-2191,757) and rno-miR-206 (miRBase MI0000948, Chromosome 9: 19,401,985-19,402,068), three potential SRF recognition elements (REs) in 5′UTR sequence of rno-miR-1 and five potential SRF REs in 5′UTR sequence of rno-miR-206 were identified. Oligonucleotides were designed and synthesized to anneal to DNA containing each SRF RE (Supplementary Table 1). The annealing DNA fragments with sticky ends were inserted into the pGL3-enhancer vector to construct recombinant luciferase reporter plasmids for rno-miR-1 or rno-miR-206 transcription activity assays.

Rat H9c2 cardiomyocytes (3×10^5 cells per well) were plated in 12-well plates 24 h before transfection. Cells were co-transfected with 1 μg of rno-miR-1 reporter plasmid or rno-miR-206 reporter plasmid, and 20 ng of pRL-TK (Promega) was used as an internal control for cell viability and transfection efficiency. Activities of firefly luciferase and RL were measured 48 h after transfection and incubation with 25 mM glucose in media; the relative ratio of the firefly luciferase/RL was used for calculation of miR-1 or miR-206 transcription activities.

2.7. Constructions of miR-1/miR-206 sponge expression plasmid

As an alternative to chemically-modified antisense oligonucleotides, a miR-1/miR-206 sponge expression plasmid was constructed to block miR-1/miR-206 function. To construct the miR-1/miR-206 sponge expression plasmid, four repeats of the binding sequence (5′-AATAAAGACATTTGTACATTCCT-3′) of rat miR-1 and miR-206 in the 3′-untranslated region of the rat *Hsp60* gene were tandemly

inserted into the multiple cloning site (between the *Hin*dIII and *Eco*RI sites) of pcDNA3. The recombinant plasmid, pcDNA3-miR-1/miR-206-sponge, was identified by DNA sequencing.

2.8. Cell culture and transfection

Neonatal rat ventricular cardiomyocytes (NRVCs) were isolated from the hearts of new-born SD rats as described previously [31]. Isolated NRVCs were plated onto 12-well plates and maintained for 48 h in Dulbecco's Modified Eagle's Medium (DMEM)/F-12 supplemented with 10% fetal bovine serum (FBS) (GIBCO, New York, USA). The cells were serum-starved overnight prior to all experiments. NRVCs were transfected with miR-1 mimics and/or miR-206 mimics (Genpharma, Shanghai, China) using Oligofectamine reagent (Invitrogen).

H9c2 rat myoblasts were cultured in DMEM supplemented with 10% FBS at 37 °C and 5% CO_2. H9c2 cells were transfected with pcDNA3, pcDNA3-miR-1, pcDNA3-miR-206, pcDNA3-miR-1/miR-206-sponge, or pcDNA3-*Hsp60*/miR155-shRNA using Lipofectamine 2000 reagent (Invitrogen). After 48 h, Geneticin (G418) (Invitrogen)was added to the culture medium at a concentration of 600 μg/ml for screening and 300 μg/ml for amplification of transfected cells. pcDNA3 and pcDNA3-miR-1/miR-206-sponge were also transfected into HEK293 cells to establish the corresponding stable cell lines using the previously mentioned methods.

2.9. Real-time quantitative PCR

Total cellular RNAs were extracted using Trizol reagent (Gibco-BRL). First-strand cDNAs were synthesized using a mixture of

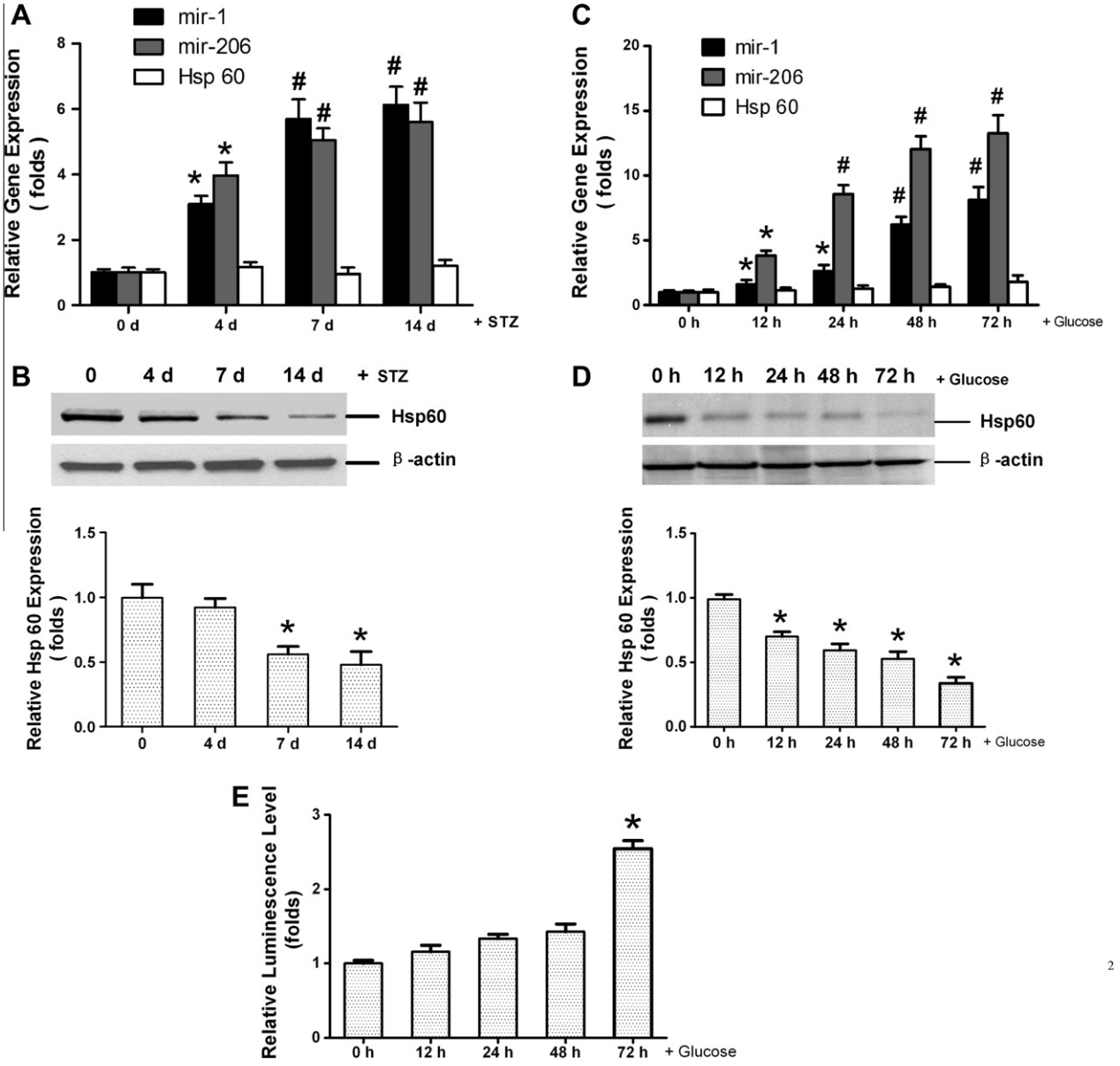

Fig. 1. Analysis of miR-1 and miR-206 precursor transcripts and Hsp60 mRNA and protein and glucose-induced apoptosis. miR-1 and mir-206 precursors transcripts and Hsp60 mRNA expression was detected using real-time quantitative PCR, and Hsp 60 protein expression was analyzed using Western blot analysis. miR-1 and mir-206 precursors transcripts and Hsp 60 mRNA (A) and Hsp 60 protein (B) expression were detected in diabetic rat hearts at 4, 7, and 14 d after streptozotocin (STZ) induction. miR-1 and mir-206 precursors transcripts and Hsp 60 mRNA (C) and Hsp 60 protein (D) expression were detected in neonatal rat ventricular cardiomyocytes (NRVC) exposed to 25 mM glucose for 12, 24, 48, and 72 h. Each value was expressed as the relative to the control, and the value of control was set to 1. (E) Glucose-induced NRVC apoptosis. The NRVCs were exposed to 25 mM glucose for 12, 24, 48 and 72 h after which caspase-9 activities were assessed using a homogeneous luminescent assay. $^{*}P < 0.05$ versus control, $^{\#}P < 0.01$ versus control.

oligo(dT)$_{12-18}$ primers with Superscript reverse transcriptase (Invitrogen). The real-time PCR was performed using the MJ Opticon II Quantitative PCR System (MJ Research, Waltham, MA, USA) and the following thermal cycling profile: 95 °C for 5 min, followed by 40 cycles of amplification (94 °C for 20 s, 58 °C for 25 s, and 72 °C for 25 s). The absorption values of the SYBR Green I fluorescence in each tube were detected at the end of each cycle. The housekeeping gene encoding *β-actin* was used as an internal control. The following specific primers were used in the real-time PCR reaction: miR-1-forward, 5′-TCAATCTCTAACAAGCTAATCTCT-3′ and miR-1-reverse, 5′-TTGACAGTAGGTTAATCCAAAGT-3′ (296 bp); miR-206-forward, 5′-CAAGATGGCGACTTACGGATG-3′ and miR-206-reverse, 5′-CTGCAGGTAGGACAAACGTG-3′ (288 bp); *Hsp60*-forward, 5′-CTGCAATGACAATTGCTAAGAA-3′ and *Hsp60*-reverse, 5′-ATTCCAGGGTCCTTCTCTTCT-3′ (250 bp); *SRF*-forward, 5′-CAGCCTCACCGTGCTCAATG-3′ and *SRF*-reverse, 5′-TCATTCACTCTT GGTGCTGTG-3′ (250 bp); and *β*-actin–forward, 5′-GCCAACACAGTG CTGTCTG-3′ and *β-actin*-reverse, 5′-TACTCCTGCTTGCTGATCCA-3′ (203 bp). The relative expression values of miR-1 and miR-206 transcripts as well as *HSP60* and *SRF* mRNAs were calculated using $2^{-\Delta\Delta Ct}$ method [32].

2.10. Western blot analysis

The protein extract (30 μg) prepared from a tissue sample or NRVC or H9c2 cells was separated by 12% SDS–PAGE and transferred to a polyvinylidene fluoride (PVDF) membrane. The membrane was blocked with 5% milk in Tris-buffer saline solution (pH 7.6) containing 0.05% Tween-20 (TBS/T), and incubated with high affinity antibody to Hsp60 (1:1000) (Santa Cruz, Santa Cruz, CA, USA), or with high affinity antibody to P-ERK1/2 (1:500), ERK1/2 (1:500) (Cell Signaling Technology, MA, USA) overnight at 4 °C. The following day the membrane was incubated with horseradish peroxidase (HRP)-conjugated secondary antibody (Santa Cruz) for 1 h at room temperature. The immunoreactive proteins were visualized using ECL plus detection reagents (GE Healthcare, London, UK). The membranes were immunoblotted with β-actin antibody (1:1000) (Santa Cruz, USA) as an internal loading control.

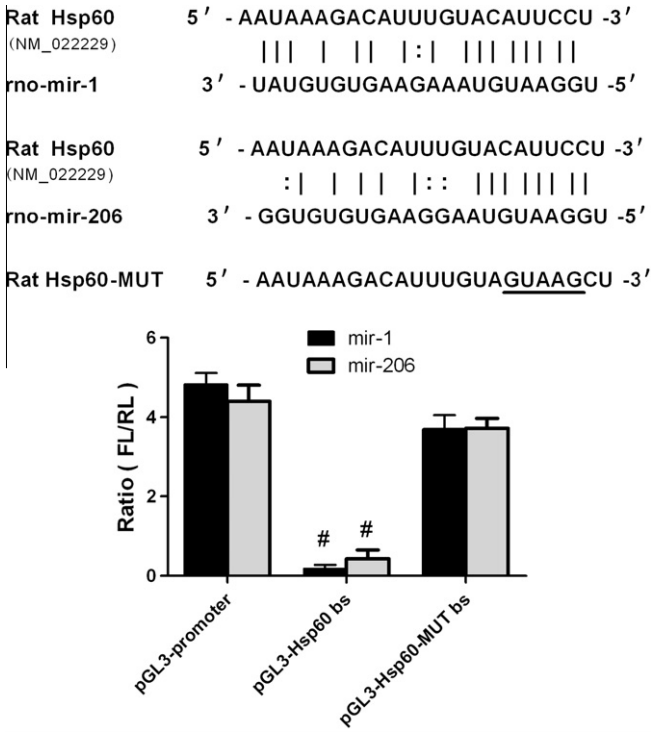

Fig. 2. miR-1 and miR-206 target Hsp60. The effect of miR-1 and miR-206 on Hsp60 was determined using the dual luciferase reporter system. The miRNA:mRNA complementary sites between the mature sequences of miR-1 and miR-206 and the 3′UTR of *Hsp 60* gene are indicated. The matched base pairs are connected by a vertical line, and the G:U/U:G wobble is indicated by dots. The GenBank accession number for the *Hsp 60* gene is indicated in brackets, and the mutated nucleotides in the target sites are underlined. *$P < 0.05$ versus pGL3-promoter vector control.

2.11. Caspase-9 activity assay

The activity of caspase-9 was determined using a Caspase-9 Assay Kit (Promega). NRVC and H9C2 cells were collected in lysis buffer with proteasome inhibitor MG-132 (Promega) and used for caspase-9 activity assay according to manufacturer's instructions.

2.12. Quantification of fragmented DNA in cell death by ELISA

DNA fragmentation in cell death was analyzed using a cell death detection ELISA kit (Roche, Mannheim, Germany) according to the manufacturer's instructions. To determine the effect of glucose on apoptosis, H9c2 cells in each groups were exposed to 25 mM glucose for 72 h. After glucose exposure, cells were lysed in 100 μL of lysis buffer and centrifuged for 10 min at 1500 rpm. DNA fragmentation was quantified by measuring absorbance at 405 nm with a reference wavelength at 492 nm.

2.13. Statistical analysis

Data represent the mean ± standard deviation (S.D.). In each experiment, all determinations were performed at least in triplicate. Differences between the experimental groups were analyzed using the Student's *t*-test. A value of $P < 0.05$ indicated significance.

3. Results

3.1. Decreased heart function in STZ-induced SD rats

One week after STZ induction, rat body weight decreased significantly with high plasma glucose levels (random glucose >16.7 mM; Data not shown). Echocardiography revealed that LVDd and LVDs were significantly increased, and EF was significantly reduced 2 weeks after STZ induction ($P < 0.05$; Supplementary Table 2). Compared with the normal controls, apoptotic cardiomyocytes significantly increased 4 d after STZ induction and in a time-dependent manner (Supplementary Fig. 1).

3.2. Up-regulation of miR-1 and miR-206 and down-regulation of Hsp60 protein in diabetic hearts and high glucose-treated NRVCs

miR-1 and miR-206 precursors as well as Hsp60 mRNA and protein was observed in rat myocardium at 4, 7, and 14 d after STZ induction. miR-1 and miR-206 expressions increased significantly in diabetic rat myocardium as compared to the normal control ($P < 0.05$; Fig. 1A). *Hsp60* mRNA levels did not change significantly in diabetic rat myocardium (Fig. 1A); however, Hsp60 protein decreased significantly at 7 and 14 d after onset of hyperglycemia ($P < 0.05$; Fig. 1B).

NRVCs were cultured and incubated with 25 mM glucose in vitro. Quantitative PCR results showed that both miR-1 and miR-206 were significantly up-regulated in a time-dependent manner in glucose-treated NRVCs ($P < 0.05$; Fig. 1C); *Hsp60* mRNA levels were not significantly altered in response to glucose treatment (Fig. 1C) as compared with normal control. Hsp60 protein decreased significantly in glucose-treated NRVCs in a time-dependent manner ($P < 0.05$; Fig. 1D). Furthermore, caspase-9

activity was significantly elevated in NRVCs treated with high glucose for 72 h ($P < 0.05$; Fig. 1E).

3.3. Post-transcriptional repression of Hsp60 by miR-1 and miR-206

A bioinformatics-based approach was employed to predict the putative targets using the TargetScan program hosted by the Wellcome Trust Sanger Institute [33]. One potential binding site was found in the 3′UTR of rat *Hsp 60* gene for rat miR-1 and miR-206 (Fig. 2), and one similar potential binding site was found in the 3′UTR of human *Hsp* 60 gene for huamn miR-1 and miR-206 (Supplementary Fig. 2). The dual luciferase assay demonstrated that miR-1 and miR-206 significantly reduced the luciferase activities mediated by pGL3-Hsp60 bs ($P < 0.05$), but not pGL3-Hsp60-MUT bs (Fig. 2).

The effects of miR-1 on Hsp60 expression in the stable H9C2 cells was also investigated. Whereas high glucose up-regulated miR-1 precursor transcripts ($P < 0.05$; Fig. 3A), it did not alter *Hsp60* mRNA (Fig. 3B). *Hsp60* mRNA was significantly reduced by *Hsp60* shRNA, but was unaffected by over-expression of

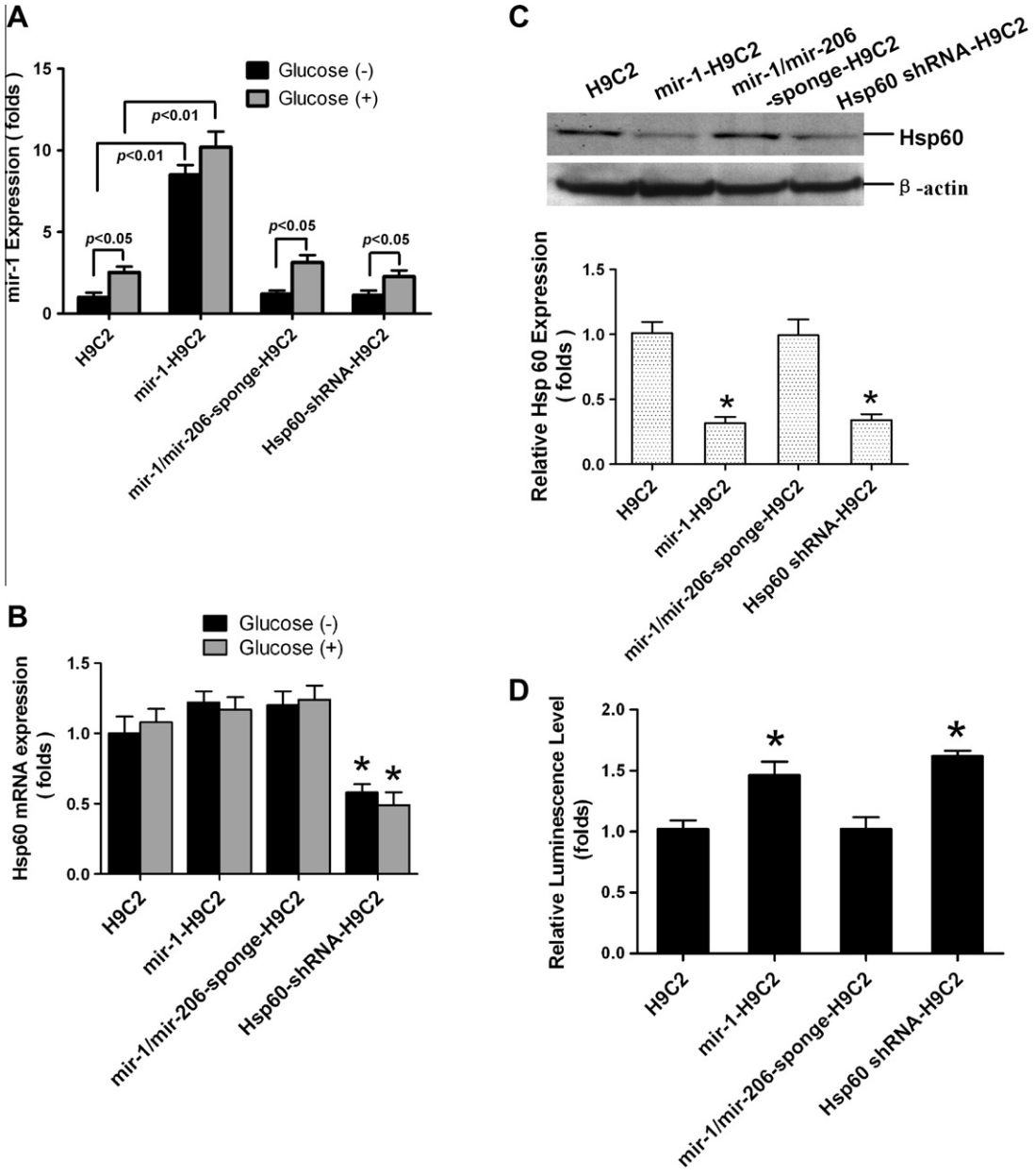

Fig. 3. Effects of high glucose on miR-1 precursor transcript and Hsp60 expression and effects of miR-1 and miR-206 mimics on Hsp 60 expression. (A and B) The expression of miR-1 precursor transcript and Hsp 60 mRNA was examined by real-time quantitative PCR in the stable H9C2 cells with or without exposure to 25 mM glucose for 24 h. (C) Hsp 60 protein expression was detected using Western blot analysis of the stable H9C2 cells. (D) Caspase-9 activities in the stable H9C2 cells induced with 25 mM glucose for 48 h. Each value was expressed as the ratio of caspase-9 activation to that observed in the control group (H9C2 cells transfected with pcDNA3), and the value of control was set to 1. (E) Glucose-induced H9C2 cell apoptosis. The stable H9C2 cells were exposed to 25 mM glucose for 72 h, and cells were assessed for apoptosis by analyzing histone-associated DNA fragments. Hsp 60 mRNA (F) and Hsp 60 protein (G) expression were detected in NRVCs transfected with 50 nM Duplex, 50 nM miR-1 mimics and 25 nM miR-1 mimics plus 25 nM miR-206 mimics for 48 h. Each value was expressed as the relative to the Duplex control, and the value of control was set to 1. β-actin served as an internal control in the real-time quantitative PCR and Western blot analyses (A–C, F and G). (H) Caspase-9 activities in NRVCs transfected with corresponding mimics (shown in F and G) after incubation with 25 mM glucose for 48 h. Each value was expressed as the ratio of caspase-9 activation to that observed in the control group (NRVCs transfected with Duplex control), and the value of control was set to 1. $^{*}P < 0.05$ versus control, $^{\#}P < 0.01$ versus control.

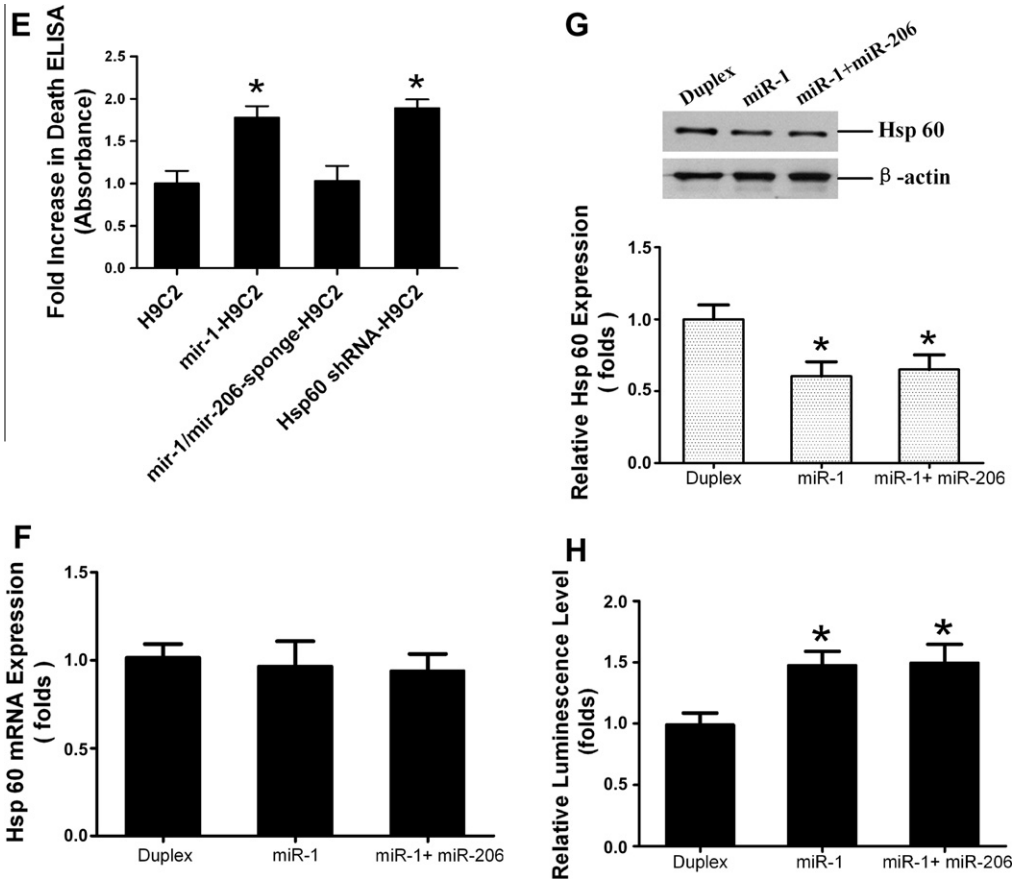

Fig. 3 (*continued*)

miR-1 in the mir-R-1-stable H9C2 cells (Fig. 3 B), indicating that miR-1 does not affect *Hsp60* mRNA stability. Consistent results were also observed in the miR-206-stable H9C2 cells (Data not shown).

Western blot analysis revealed that miR-1 and miR-206 significantly reduced Hsp60 protein to an extent similar with *Hsp60* shRNA (Fig. 3C, Supplementary Fig. 4A). In addition, miR-1/miR-206-sponge could efficiently blocked miR-1 or miR-206 activity ($P < 0.01$; Supplementary Fig. 3), and specifically reversed Hsp60 protein reduction mediated by miR-1 or miR-206 (Fig. 3C, Supplementary Fig. 4A).

50 nM miR-1 mimics and 25 nM miR-1 mimics plus 25 nM miR-206 mimics could efficiently suppressed Hsp 60 protein expression to the similar extent, without obvious effects on Hsp 60 mRNA expression ($P < 0.05$; Fig. 3F and G).

3.4. miR-1 and miR-206 mediate their effects on H9c2 cell apoptosis through Hsp60

Caspase-9 activities were significantly increased in H9c2 cells transfected with miR-1/miR-206 or Hsp60 shRNA after 48 h exposure to 25 mM glucose ($P < 0.05$); no obvious elevations in caspase-9 activities were observed in H9C2 cells transfected with miR-1/miR-206-sponge (Fig. 3D, Supplementary Fig. 4B). Consistent results were observed in cell death ELISA assays of the stable H9c2 cells exposed to high glucose for 72 h (Fig. 3E, Supplementary Fig. 4C). TUNEL assay also showed that the percentage of apoptotic cells increased significantly in high glucose-induced H9C2 cells modified with miR-1 or Hsp60 shRNA ($P < 0.05$), and miR-1/miR-206 sponge specifically inhibited high glucose-induced H9c2 cell apoptosis (Supplementary Fig. 5).

Caspase-9 activities were similarly and significantly increased in NRVCs transfected with 50 nM miR-1 mimics and in NRVCs transfected with 25 nM miR-1 mimics plus 25 nM miR-206 mimics after 48 h exposure to 25 mM glucose ($P < 0.05$; Fig. 3H).

3.5. The MEK1/2 pathway and SRF transcription factor mediate miR-1/miR-206 expression in cardiomyocytes induced by glucose

SRF mRNA expression was observed in H9c2 cells after 12, 24, 36, and 72 h exposure to high glucose. Quantitative real-time PCR showed that SRF mRNA was significantly up-regulated by glucose in a time-dependent manner (Supplementary Fig. 6).The Dual luciferase assay revealed that three SRF REs in the 5′UTR of rno-miR-1 mediated miR-1 expression, and SRF RE2, RE3, RE4, and RE5 mediated miR-206 expression in H9c2 cells induced with high glucose (Fig. 4A). In addition, SRF shRNA efficiently inhibited miR-1 and miR-206 transcriptional activity (Data not shown) and reduced their levels in H9c2 cells ($P < 0.05$; Fig. 4B). Quantitative real-time PCR analysis revealed that the MEK1/2 inhibitor, PD98059, inhibited miR-1 and miR-206 expression induced by glucose in H9c2 cells ($P < 0.05$; Fig. 4C). The activity of ERK1/2 was significantly increased in 25 mM glucose-treated NRVCs within 30–120 min, and peak levels were observed at 60 min (Fig. 4D). IGF-1 (GroPep, Adelaide, Australia) at does of 15, 30 and 45 ng/ml could significantly inhibit mir-1 and miR-206 expression in a does-dependent manner in 25 mM glucose-treated NRVCs for 24 h (Fig. 4E). In the presence of 30 ng/ml IGF-1, mir-1 and miR-206 expression was significantly

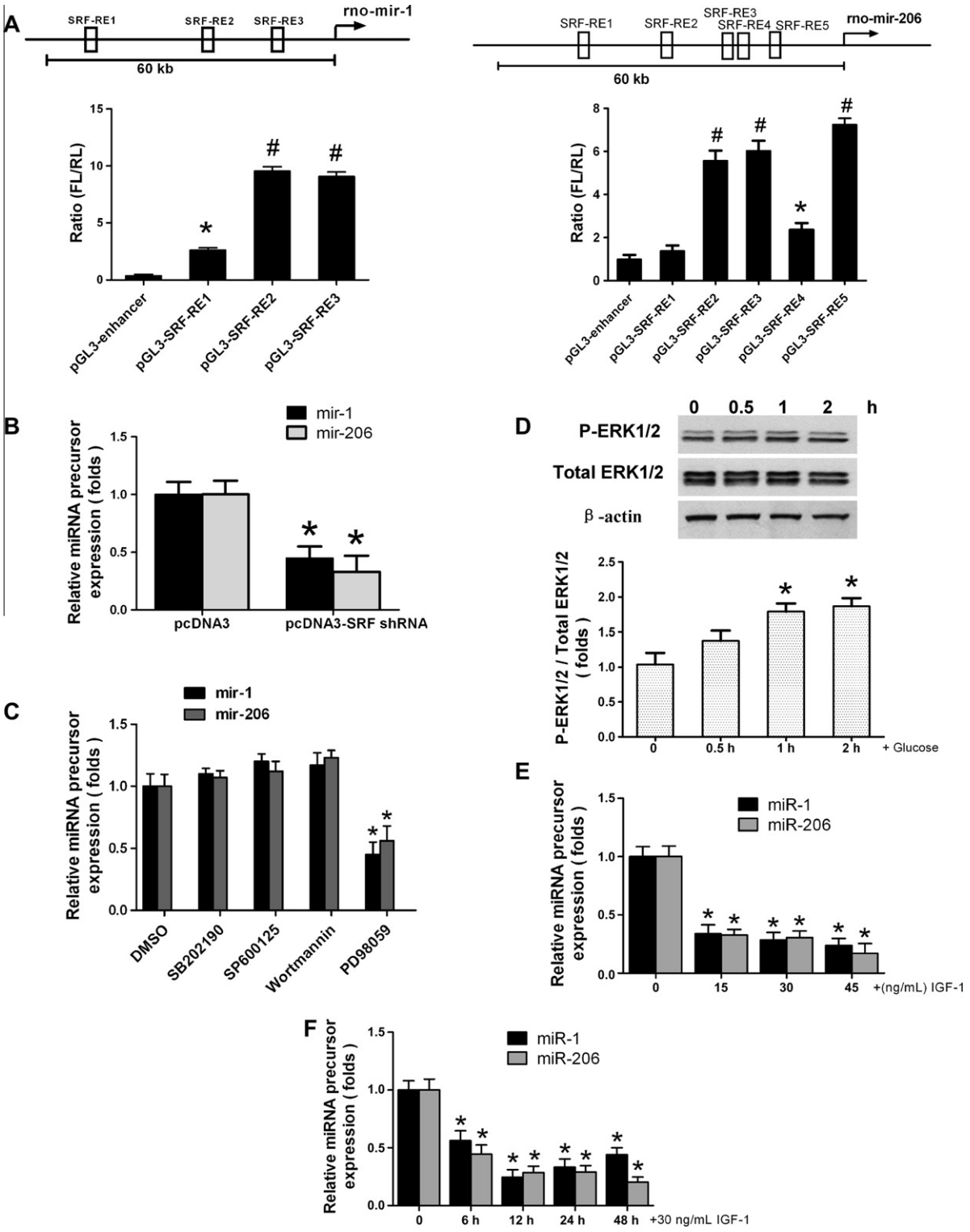

Fig. 4. The effects of SFR and IGF-1 on high glucose-induced miR-1 and miR-206 expression. (A) The luciferase activities in H9C2 cells transfected with eight different pGL3-SRF-RE promoter plasmids and incubated with 25 mM glucose. Three potential SRF recognition elements (SRF-RE) were predicted in the 60 kb 5′ UTR of the rat miR-1 and five were predicted in the 60 kb 5′ UTR of the rat miR-206 (schematic). H9C2 cells transfected with the pGL3-promoter were used as a control group. (B) The expression of miR-1 and miR-206 precursor transcripts were examined by real-time quantitative PCR in the SRF shRNA-transfected H9C2 cells incubated with 25 mM glucose for 24 h. H9C2 cells transfected with pcDNA3 vector were used as the control group. (C) The expression of miR-1 and miR-206 precursor transcripts were examined by real-time quantitative PCR in H9C2 cells incubated with 25 mM glucose and SB202190, SP600125, Wortmannin, or PD98059 for 24 h. H9C2 cells incubated with 25 mM glucose and DMSO were used as the control group. (D) Analysis of time course of 25 mM glucose treatment on protein level of activated p-ERK1/2, with total ERK1/2 used as a control, in NRVCs. The expression of miR-1 and miR-206 precursors was examined by real-time quantitative PCR in NRVCs with exposure to 25 mM glucose plus 0, 15, 30 and 45 ng/ml IGF-1 for 24 h (E), and in NRVCs with exposure to 25 mM glucose plus 30 ng/ml IGF-1 for 0, 6, 12 and 24 h, respectively (F). β-actin served as an internal control in the real-time quantitative PCR assays in (B, E, and F). $^{*}P < 0.05$ versus control, $^{\#}P < 0.01$ versus control.

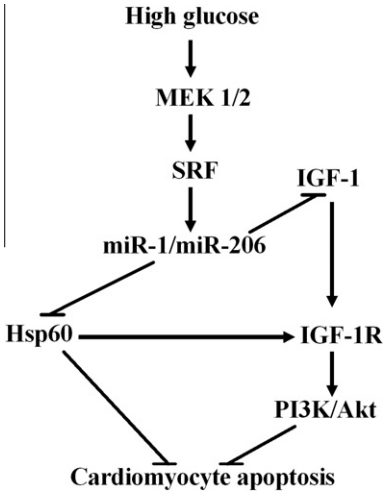

Fig. 5. miR-1/miR-206 regulate Hsp60 and IGF-1 expression, contributing to glucose-mediated apoptosis in cardiomyocytes. A schematic diagram for the role of miR-1 /miR-206 in Hsp 60 and IGF-1 reduction induced by high glucose is shown. Up-regulation of miR-1/miR-206 by high glucose through the MEK1/2-SRF pathway ERK1/2SRF results in suppression of Hsp 60 and IGF-1 expression and inhibition of IGF-1/IGF-1R/PI3 K/Akt pathway, contributing to high glucose-mediated cardiomyocyte apoptosis.

suppressed in 25 mM glucose-treated NRVCs for 6, 12, 24 or 48 h (Fig. 4F).

4. Discussion

We previously reported that high glucose promoted miR-1 expression in rat cardiac H9c2 cells [27]. In the present study, miR-1 and miR-206 were up-regulated in the myocardium after onset of hyperglycemia and in neonatal ventricular cardiomyocytes and H9c2 cells after exposure to high glucose. This result is also consistent with a previous study that reported increased miR-1 expression in ventricular samples from diabetic patients [26]. The present study showed increased apoptotic cardiomyocytes in the diabetic myocardium in a time-dependent manner, and cardiac function was decreased in STZ-induced SD rats with increased apoptotic cardiomyocytes. Increased apoptosis was also found in high glucose-treated cardiomyocytes in a time-dependent manner. Because blocking miR-1 or miR-206 function using the miR-1/miR-206 sponge inhibited cardiac cells apoptosis, up-regulation of miR-1 and miR-206 may contribute to high glucose-induced cardiac cell apoptosis. SRF was also up-regulated, modulating miR-1 and miR-206 expression in cardiomyocytes exposed to high glucose. This observation is consistent with a previous report that SRF regulates miR-1 expression during cardiogenesis [30]. High glucose activated ERK1/2, and using the MEK1/2 inhibitor, PD98059, could inhibit of both miR-1 and miR-206 expression in cardiomyocytes exposed to high glucose. These results indicate that blocking SRF or the MEK1/2 pathway may present a novel method to inhibit miR-1 and miR-206 expression in the diabetic myocardium.

Both miR-1 and miR-206 modulated Hsp60 expression in cardiac cells post-transcriptionally, which is consistent with a report that miR-1 suppresses Hsp60 expression in H9c2 cells under oxidative stress [34]. However, no additive effects of miR-1 and miR-206 on Hsp 60 expression and cardiomyocyte apoptosis were found in this study, the potential reason is that miR-1 and miR-206 share an identical seed sequence to bind to the same site in the 3′-UTR of Hsp 60 mRNA (Fig. 2).

Hsp60 is an anti-apoptotic protein, which can be constitutively and inducibly expressed in mammalian tissues. Hsp60 can form complexes with Bax, Bak, and Bcl-xS [7,9,10], preventing Bax oligomerization and insertion into the mitochondrial membrane, and therefore avoiding the mitochondrial apoptotic pathway. In the present study, we confirmed that Hsp60 protein was reduced in the diabetic myocardium as well as high glucose-treated cardiomyocytes, which is consistent with previous reports [11–14]. In addition, cell apoptosis levels were increased in the H9c2 cells modified with Hsp60 shRNA, miR-1 or miR-206. Thus, miR-1 and miR-206 regulate Hsp60 expression, thereby contributing to glucose-mediated apoptosis in cardiomyocytes.

IGF-1 [27,35,36] and Hsp60 [7,9,10] protect the myocardium against apoptosis through the mitochondrial pathway. Our previous study showed that IGF-1 could abrogate high glucose-induced apoptosis of rat H9c2 cardiomyocytes and IGF-1 mediated the effect of miR-1 contributing to high glucose-induced H9c2 apoptosis [27]. In the present study, we further demonstrated that IGF-1 could efficiently suppressed both miR-1 and miR-206 expression in cardiomyocytes exposed to high glucose concentration. This result revealed that inhibiting miR-1 and miR-206 expression is a new mechanism for the effect of IGF-1 in protecting cardiomyocytes against high glucose-induced apoptosis.

Down-regulation of cytoplasmic Hsp60 contributes to IGF-1 receptor (IGF-1R) ubiquitination [14]. As predicted by the microRNA bioinformatics program (http://www.microrna.org), a potential target site (6895–6916) in the 3′-UTR of the human *IGF1R* gene (GenBank accession, NM_000875) for human miR-1 and miR-206, and a potential target site (5246–5267) in the 3′-UTR of the mouse *IGF1R* gene (GenBank accession, NM_010513) for mouse miR-1 and miR-206 were found (data not shown). A recent study showed that IGF-1R, phosphatidylinositol 3′-kinase (PI3 K), and the protein kinase B (Akt) were significantly decreased in type 1-like diabetic rats [37]. Therefore, the present findings suggest that up-regulation of miR-1 and miR-206 contribute to high glucose-induced cardiomyocyte apoptosis via two pathways. Firstly, miR-1 and miR-206 suppress Hsp60 expression, and reduced Hsp60 contributes to *IGF1R* degradation. Secondly, miR-1 and miR-206 inhibit IGF-1/IGF-1R/PI3 K/AKt signaling pathway (Fig. 5).

In summary, the present study revealed a new pathway for post-transcriptional control of Hsp60 in cardiomyocytes exposed to high glucose. Specifically, high glucose stimulates miR-1 and miR-206 expression through the MEK1/2 pathway and SRF, and up-regulation of miR-1 and miR-206 suppress Hsp60 expression, contributing to high glucose-mediated cardiomyocyte apoptosis.

Acknowledgements

This work was supported by Grants from the National Natural Science Foundation of China (Nos. 30672077, 30772142) and the National Key Basic Research Program (NKBRP) of China (No. 2006CB503806).

Appendix A. Supplementary data

Supplementary data associated with this article can be found, in the online version, at doi:10.1016/j.febslet.2010.07.027.

References

[1] Rota, M., LeCapitaine, N., Hosoda, T., Boni, A., De Angelis, A., Padin-Iruegas, M.E., Esposito, G., Vitale, S., Urbanek, K., Casarsa, C., Giorgio, M., Luscher, T.F., Pelicci, P.G., Anversa, P., Leri, A. and Kajstura, J. (2006) Diabetes promotes cardiac stem cell aging and heart failure, which are prevented by deletion of the p66shc gene. Circ. Res. 99, 42–52.
[2] Yoon, Y.S., Uchida, S., Masuo, O., Cejna, M., Park, J.S., Gwon, H.C., Kirchmair, R., Bahlman, F., Walter, D., Curry, C., Hanley, A., Isner, J.M. and Losordo, D.W.

(2005) Progressive attenuation of myocardial vascular endothelial growth factor expression is a seminal event in diabetic cardiomyopathy: restoration of microvascular homeostasis and recovery of cardiac function in diabetic cardiomyopathy after replenishment of local vascular endothelial growth factor. Circulation 111, 2073–2085.
[3] Yu, T., Robotham, J.L. and Yoon, Y. (2006) Increased production of reactive oxygen species in hyperglycemic conditions requires dynamic change of mitochondrial morphology. Proc. Natl. Acad. Sci. USA. 103, 2653–2658.
[4] Yu, T., Sheu, S.S., Robotham, J.L. and Yoon, Y. (2008) Mitochondrial fission mediates high glucose-induced cell death through elevated production of reactive oxygen species. Cardiovasc. Res. 79, 341–351.
[5] Ding, H., Hashem, M. and Triggle, C. (2007) Increased oxidative stress in the streptozotocin-induced diabetic apoE-deficient mouse: changes in expression of NADPH oxidase subunits and Enos. Eur. J. Pharmacol. 561, 121–128.
[6] Gupta, S. and Knowlton, A.A. (2005) HSP60, Bax, apoptosis and the heart. J. Cell. Mol. Med. 9, 51–58.
[7] Kirchhoff, S.R., Gupta, S. and Knowlton, A.A. (2002) Cytosolic heat shock protein 60, apoptosis, and myocardial injury. Circulation 105, 2899–2904.
[8] Lau, S., Patnaik, N., Sayen, M.R. and Mestril, R. (1997) Simultaneous overexpression of two stress proteins in rat cardiomyocytes and myogenic cells confers protection against ischemia-induced injury. Circulation 96, 2287–2294.
[9] Lin, K.M., Lin, B., Lian, I.Y., Mestril, R., Scheffler, I.E. and Dillmann, W.H. (2001) Combined and individual mitochondrial HSP60 and HSP10 expression in cardiac myocytes protects mitochondrial function and prevents apoptotic cell deaths induced by simulated ischemia-reoxygenation. Circulation 103, 1787–1792.
[10] Shan, Y.X., Liu, T.J., Su, H.F., Samsamshariat, A., Mestril, R. and Wang, P.H. (2003) Hsp10 and HSP60 modulate Bcl-2 family and mitochondria apoptosis signaling induced by doxorubicin in cardiac muscle cells. J. Mol. Cell. Cardiol. 35, 1135–1143.
[11] Turko, I.V. and Murad, F. (2003) Quantitative protein profiling in heart mitochondria from diabetic rats. J. Biol. Chem. 278, 35844–35849.
[12] Shan, Y.X., Yang, T.L., Mestril, R. and Wang, P.H. (2003) Hsp10 and Hsp60 suppress ubiquitination of insulin-like growth factor-1 receptor and augment insulin-like growth factor-1 receptor signaling in cardiac muscle: implications on decreased myocardial protection in diabetic cardiomyopathy. J. Biol. Chem. 278, 45492–45498.
[13] Chen, H.S., Shan, Y.X., Yang, T.L., Lin, H.D., Chen, J.W., Lin, S.J. and Wang, P.H. (2005) Insulin deficiency downregulated heat shock protein 60 and IGF-1 receptor signaling in diabetic myocardium. Diabetes 54, 175–181.
[14] Lai, H.C., Liu, T.J., Ting, C.T., Yang, J.Y., Huang, L., Wallace, D., Kaiser, P. and Wang, P.H. (2007) Regulation of IGF-I receptor signaling in diabetic cardiac muscle: dysregulation of cytosolic and mitochondria HSP60. Am. J. Physiol. Endocrinol. Metab. 292, E292–E297.
[15] Karp, X. and Ambros, V. (2005) Developmental biology: encountering microRNAs in cell fate signaling. Science 310, 1288–1289.
[16] Kloosterman, W.P. and Plasterk, R.H. (2006) The diverse functions of microRNAs in animal development and disease. Dev. Cell. 11, 441–450.
[17] van Rooij, E., Sutherland, L.B., Liu, N., Williams, A.H., McAnally, J., Gerard, R.D., Richardson, J.A. and Olson, E.N. (2007) A signature pattern of stress-responsive microRNAs that can evoke cardiac hypertrophy and heart failure. Proc. Natl. Acad. Sci. USA 103, 18255–18260.
[18] Kim, J., Inoue, K., Ishii, J., Vanti, W.B., Voronov, S.V., Murchison, E., Hannon, G. and Abeliovich, A. (2007) A microRNA feedback circuit in midbrain dopamine neurons. Science 317, 1220–1224.
[19] Calin, G.A. and Croce, C.M. (2006) MicroRNA signatures in human cancers. Nat. Rev. Cancer 6, 857–866.
[20] Li, Y., Song, Y.H., Li, F., Yang, T., Lu, Y.W. and Geng, Y.J. (2009) MicroRNA-221 regulates high glucose-induced endothelial dysfunction. Biochem. Biophys. Res. Commun. 381, 81–83.
[21] Horie, T., Ono, K., Nishi, H., Iwanaga, Y., Nagao, K., Kinoshita, M., Kuwabara, Y., Takanabe, R., Hasegawa, K., Kita, T. and Kimura, T. (2009) MicroRNA-133 regulates the expression of GLUT4 by targeting KLF15 and is involved in metabolic control in cardiac myocytes. Biochem. Biophys. Res. Commun. 389, 315–320.
[22] Lu, H., Buchan, R.J. and Cook, S.A. (2010) MicroRNA-223 regulates Glut4 expression and cardiomyocyte glucose metabolism. Cardiovasc. Res. 86, 410–420.
[23] Yang, B., Lin, H., Xiao, J., Lu, Y., Luo, X., Li, B., Zhang, Y., Xu, C., Bai, Y., Wang, H., Chen, G. and Wang, Z. (2007) The muscle-specific microRNA miR-1 regulates cardiac arrhythmogenic potential by targeting GJA1 and KCNJ2. Nat. Med. 13, 486–491.
[24] Thum, T., Galuppo, P., Wolf, C., Fiedler, J., Kneitz, S., van Laake, L.W., Doevendans, P.A., Mummery, C.L., Borlak, J., Haverich, A., Gross, C., Engelhardt, S., Ertl, G. and Bauersachs, J. (2007) MicroRNAs in the human heart: a clue to fetal gene reprogramming in heart failure. Circulation 116, 258–267.
[25] Chen, J.F., Mandel, E.M., Thomson, J.M., Wu, Q., Callis, T.E., Hammond, S.M., Conlon, F.L. and Wang, D.Z. (2006) The role of microRNA-1 and microRNA-133 in skeletal muscle proliferation and differentiation. Nat. Genet. 38, 228–233.
[26] Xiao, J., Luo, X., Lin, H., Zhang, Y., Lu, Y., Wang, N., Zhang, Y., Yang, B. and Wang, Z. (2007) MicroRNA miR-133 represses HERG K+ channel expression contributing to QT prolongation in diabetic hearts. J. Biol. Chem. 282, 12363–12367.
[27] Yu, X.Y., Song, Y.H., Geng, Y.J., Lin, Q.X., Shan, Z.X., Lin, S.G. and Li, Y. (2008) Glucose induces apoptosis of cardiomyocytes via microRNA-1 and IGF-1. Biochem. Biophys. Res. Commun. 76, 548–552.
[28] Shan, Z.X., Lin, Q.X., Fu, Y.H., Deng, C.Y., Zhou, Z.L., Zhu, J.N., Liu, X.Y., Zhang, Y.Y., Li, Y., Lin, S.G. and Yu, X.Y. (2009) Upregulated expression of miR-1/miR-206 in a rat model of myocardial infarction. Biochem. Biophys. Res. Commun. 381, 597–601.
[29] Shan, Z.X., Lin, Q.X., Yang, M., Deng, C.Y., Kuang, S.J., Zhou, Z.L., Xiao, D.Z., Liu, X.Y., Lin, S.G. and Yu, X.Y. (2009) A quick and efficient approach for gene silencing by using triple putative microRNA-based short hairpin RNAs. Mol. Cell. Biochem. 323, 81–89.
[30] Zhao, Y., Samal, E. and Srivastava, D. (2005) Serum response factor regulates a muscle-specific microRNA that targets Hand2 during cardiogenesis. Nature 14 (436), 214–220.
[31] Liu, N., Williams, A.H., Kim, Y., McAnally, J., Bezprozvannaya, S., Sutherland, L.B., Richardson, J.A., Bassel-Duby, R. and Olson, E.N. (2007) An intragenic MEF2-dependent enhancer directs muscle-specific expression of microRNAs 1 and 133. Proc. Natl. Acad. Sci. USA 104, 20844–20849.
[32] Pfaffl, M.W. (2001) A new mathematical model for relative quantification in real-time RT-PCR. Nucleic Acids Res. 29, e45.
[33] Griffiths-Jones, S. (2004) The microRNA registry. Nucleic Acids Res. 32, D109–D111.
[34] Xu, C., Lu, Y., Pan, Z., Chu, W., Luo, X., Lin, H., Xiao, J., Shan, H., Wang, Z. and Yang, B. (2007) The muscle-specific microRNAs miR-1 and miR-133 produce opposing effects on apoptosis by targeting HSP60, HSP70 and caspase-9 in cardiomyocytes. J. Cell. Sci. 120, 3045–3052.
[35] Li, Y., Higashi, Y., Itabe, H., Song, Y.H., Du, J. and Delafontaine, P. (2003) Insulin-like growth factor-1 receptor activation inhibits oxidized LDL-induced cytochrome-c release and apoptosis via the phosphatidylinositol 3 kinase/Akt signalling pathway. Arterioscler. Thromb. Vasc. Biol. 23, 2178–2184.
[36] Delafontaine, P., Song, Y.H. and Li, Y. (2004) Expression, regulation, and function of IGF-1, IGF-1R, and IGF-1 binding proteins in blood vessels. Arterioscler. Thromb.Vasc. Biol. 24, 435–444.
[37] Kuo, W.W., Chung, L.C., Liu, C.T., Wu, S.P., Kuo, C.H., Tsai, F.J., Tsai, C.H., Lu, M.C., Huang, C.Y. and Lee, S.D. (2009) Effects of insulin replacement on cardiac apoptotic and survival pathways in streptozotocin-induced diabetic rats. Cell. Biochem. Funct. 27, 479–487.